frontiers | Frontiers in Immunology

TYPE Original Research
PUBLISHED 12 March 2024
DOI 10.3389/fimmu.2024.1343512

OPEN ACCESS

EDITED BY
Qun Zhao,
Fourth Hospital of Hebei Medical University, China

REVIEWED BY
Kui Wang,
Shanghai Jiao Tong University, China
Mubashir Ayaz Ahmed,
AMITA Health St Joseph Hospital, United States

*CORRESPONDENCE
Ya-ming Zhang
zhangyaming2014@163.com
Yao Wang
wangyaodna@foxmail.com

RECEIVED 23 November 2023
ACCEPTED 21 February 2024
PUBLISHED 12 March 2024

CITATION
Wang Y-x, Zhou C-p, Wang D-t, Ma J, Sun X-h, Wang Y and Zhang Y-m (2024) Unraveling the causal role of immune cells in gastrointestinal tract cancers: insights from a Mendelian randomization study. *Front. Immunol.* 15:1343512. doi: 10.3389/fimmu.2024.1343512

Unraveling the causal role of immune cells in gastrointestinal tract cancers: insights from a Mendelian randomization study

Yu-xiang Wang[1], Chao-ping Zhou[1], Da-tian Wang[1], Jun Ma[1], Xue-hu Sun[2], Yao Wang[3]* and Ya-ming Zhang[1]*

[1]Department of General Surgery, Anqing Municipal Hospital, Anqing, Anhui, China, [2]Department of Emergency Surgery, The First Affiliated Hospital of Anhui Medical University, Hefei, Anhui, China, [3]Department of Digestive Endoscopy, The First Affiliated Hospital with Nanjing Medical University, Nanjing, Jiangsu, China

Background: Despite early attempts, the relationship between immune characteristics and gastrointestinal tract cancers remains incompletely elucidated. Hence, rigorous and further investigations in this domain hold significant clinical relevance for the development of novel potential immunotherapeutic targets.

Methods: We conducted a two-sample Mendelian randomization (MR) analysis using the tools available in the "TwoSampleMR" R package. The GWAS data for these 731 immune traits were sourced from the GWAS Catalog database. Concurrently, data on gastrointestinal tract cancers, encompassing malignant tumors in the esophagus, stomach, small intestine, colon, and rectum, were extracted from the FinnGen database. The immune traits subjected to MR analysis predominantly fall into four categories: median fluorescence intensities (MFI), relative cell (RC), absolute cell (AC), and morphological parameters (MP). To ensure the reliability of our findings, sensitivity analyses were implemented to address robustness, account for heterogeneity, and alleviate the impact of horizontal pleiotropy.

Results: A total of 78 immune traits causally linked to gastrointestinal tract cancers were identified, encompassing esophageal cancer (12 traits), gastric cancer (13 traits), small intestine cancer (22 traits), colon cancer (12 traits), and rectal cancer (19 traits). Additionally, 60 immune traits were recognized as protective factors associated with gastrointestinal tract cancers, distributed across esophageal cancer (14 traits), gastric cancer (16 traits), small intestine cancer (7 traits), colon cancer (14 traits), and rectal cancer (9 traits). Furthermore, it was observed that seven immune traits are causally related to gastrointestinal tract cancers in at least two locations. These traits include "CCR2 on CD14- CD16+ monocyte," "CD19 on IgD+ CD38-," "CD19 on IgD+ CD38- naive," "CD25hi CD45RA+ CD4 not Treg AC," "CD27 on unsw mem," "CD28 on CD39+ activated Treg," and "CD45 on CD4+."

Conclusion: This study elucidates a causal link between immune cells and gastrointestinal tract cancers at various sites through genetic investigation. The findings of this research open up new perspectives and resources for exploring tumor prevention strategies and immunotherapeutic targets.

KEYWORDS

tumor microenvironment, immunology, cancer, B cells, gastric cancer

1 Introduction

Gastrointestinal tract cancers, comprising malignant tumors in the esophagus, stomach, small intestine, colon, and rectum, represent ubiquitous lethal malignancies in human beings (1). Existing epidemiological evidence indicates a significant increase in the incidence of gastrointestinal tract cancers, particularly colorectal cancer and stomach cancer, among the youth population within the past three decades (1–3). The majority of these early-onset cases lack significant genetic or familial backgrounds, implicating potential critical roles of certain lifestyle, nutritional, metabolic, and environmental factors in cancer development (1). Therefore, an in-depth exploration of the associated risk factors of gastrointestinal tract cancers is of paramount importance for the prevention of gastrointestinal tract cancers, as well as for the development of potential anticancer agents.

In recent decades, growing body of evidence has demonstrated the crucial linkage between immune cells and the onset and progression of gastrointestinal tract cancers (4–7). For example, single-cell sequencing data has revealed that T lymphocytes and natural killer cells with exhaustion, regulatory T cells, alternatively activated macrophages, and tolerant dendritic cells dominate the tumor microenvironment of esophageal cancer (8). Moreover, it has been reported that tumor-associated macrophages (TAMs) polarize towards pro-inflammatory phenotype and induce gastric cancer cell apoptosis through IL6R-JAK-IL24 pathway, upon STING knockdown or 2'3'-c-GAMPSTING activation (4). The immune response of CD8+ T cells in regulating colorectal cancer has a significant impact on tumoral proliferation and metastasis (9). In rectal cancer, not only is the high intra-tumoral CD8+ cell density associated with improved overall survival, but also the high density of PD-1+ and CD8+ immune cells before treatment is significantly correlated with favorable response to neoadjuvant chemoradiotherapy (CRT) and improved recurrence-free survival (10). Moreover, it is noteworthy that immunotherapy has emerged as a potent clinical strategy for treating cancers (11). The number of approved immunotherapeutic drugs has been increasing, and many treatment modalities are currently under clinical and pre-clinical development (12). In summary, the incidence, progression, and clinical drug development of gastrointestinal tract cancers are closely related to immune cells. However, most studies only establish the correlation between immune cells and tumoral characteristics and fail to elucidate the directionality, i.e., the causal relationship, of this correlation. Therefore, it is of utmost importance to further investigate the causal relationship between immune cells and gastrointestinal tract cancers and screen potential immune cells as targets for prevention and treatment of gastrointestinal tract cancers.

Mendelian Randomization (MR) is a data analysis technique used in epidemiological research to evaluate causal inference. It applies genetic variation as an instrumental variable (IV) to estimate the causal relationship between the exposure factor and the outcome (13). MR utilizes the first and second laws of Mendelian inheritance, which state that the parental alleles are randomly assigned to the offspring during meiosis, so the relationship between the genes and the outcome is not affected by common confounding factors such as postnatal environment, socioeconomic status, and behavior. Therefore, the causal relationship inferred by MR has a reasonable temporal sequence (14).

In this study, we aimed to employ MR analysis to comprehensively investigate the causal relationship between different immune traits and gastrointestinal tract cancers. These findings provide resources and new insights for exploring potential targets for the prevention and treatment of gastrointestinal tract cancers.

2 Materials and methods

2.1 Study design

We conducted a comprehensive assessment to investigate the causal relationship between 731 immune traits, classified into seven groups (refer to Supplementary Table 1: B cell, cDC, TBNK, Treg, Myeloid cell, Maturation stages of T cell, and Monocyte), and gastrointestinal tract cancers using a two-sample MR approach (Figure 1) (15). The studied gastrointestinal tract cancers include those affecting the esophagus, stomach, small intestine, colon, and rectum. In MR analysis, genetic variants act as proxies for risk factors, necessitating IVs to adhere to three critical assumptions for

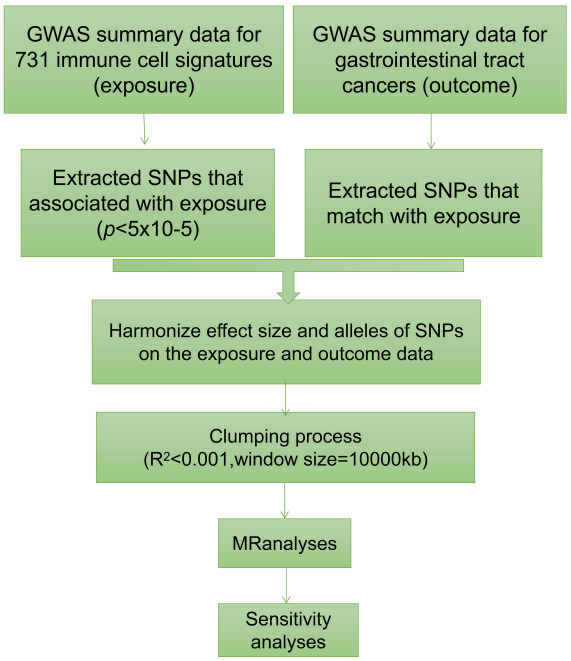

FIGURE 1
The flowchart graph of this study.

valid causal inference: (1) a direct association exists between genetic variation and the exposure of interest; (2) genetic variation remains unrelated to potential confounding variables lying between the exposure and outcome; and (3) genetic variation does not influence the outcome through pathways distinct from the exposure (16–18).

2.2 Genome-wide association study data sources

The GWAS summary statistics for total of five types of gastrointestinal tract cancers were sourced from the FinnGen database (19). Detailed information, including the number of patients and controls involved for each type of gastrointestinal tract cancer, can be found in the Supplementary Table 2. The URL for downloading the data pertaining to each type of gastrointestinal tract cancer is also incorporated in Supplementary Table 2. The diagnoses of all patients were made according to the ICD10 code. Additionally, the control group included individuals without any history of cancer.

We systematically retrieved immune trait-related signatures from the GWAS Catalog database, aiming for a comprehensive inclusion of relevant data. The final compilation encompassed a total of 731 immune traits, intricately representing diverse subsets of human immune cells (15). These signatures include absolute cell (AC) counts (n=118), median fluorescence intensities (MFI) reflecting surface antigen levels (n=389), morphological parameters (MP) (n=32), and relative cell (RC) counts (n=192).

The use of MFI, AC, and RC as quantitative or intensity units spanned various immune cell populations, including B cells, CDCs, mature stages of T cells, monocytes, myeloid cells, TBNK (T cells, B cells, natural killer cells), and Treg panels. Morphological parameters (MP) were additionally employed to represent indicators of CDC and TBNK panels.

The genetic data associated with these immune traits were sourced from 3,757 European individuals, ensuring no overlap with the GWAS data for gastrointestinal tract cancers. In the GWAS dataset, each sample underwent scrutiny for approximately 22 million single nucleotide polymorphisms (SNPs). Notably, the associations between these SNPs and the immune traits were meticulously examined, with consideration given to covariates such as sex, age, and age^2 during the analysis.

2.3 Selection of instrumental variables

Aligned with current research standards, the threshold for the significance of IVs linked to each immune trait was set at 1×10-5 (20–23). To refine the selection of SNPs, we implemented a clumping procedure, applying a linkage disequilibrium (LD) r2 threshold of less than 0.001 within a 10,000 kb distance (24–26). Subsequently, we computed F-statistics for each IV to assess their strength and mitigate potential instrumental bias. IVs with F-statistics below 10 were excluded from the analysis. This rigorous process resulted in the identification of a variable range, spanning 3 to 753 independent IVs associated with immunophenotypes, as detailed in Supplementary Table 3.

2.4 Statistical analysis

All computational analyses were performed using R 4.2.1. To assess the causal relationships between 731 immune trait-related signatures and gastrointestinal tract cancers, a comprehensive set of MR approaches, including Inverse Variance Weighting (IVW), MR Egger, Weighted Median, Simple Mode, and Weighted Mode, were executed utilizing the "TwoSampleMR" R package (version 0.5.7) (27–29).

To evaluate the presence of heterogeneity among the selected IVs, Cochran's Q statistic was applied (23). To mitigate the influence of horizontal pleiotropy, the widely recognized MR-Egger method was utilized, and the significance of its intercept term indicated potential horizontal pleiotropy (16).

To further guard against the impact of horizontal pleiotropy and the presence of potential outliers, we implemented the robust MR-Pleiotropy Residual Sum and Outlier (MR-PRESSO) method, integrated into the MR-PRESSO package (15, 23). Additionally, scatter plots and funnel plots were used for visual inspection of the data. Scatter plots confirmed resistance to the influence of outliers, while funnel plots illustrated the robustness of correlations and the absence of significant heterogeneity in the results (29).

In this study, we employed immune trait-related signatures as the exposure, and five different types of gastrointestinal tract cancer

as the outcome, for conducting MR analysis. The IVW method was utilized as the primary analysis method in our study. We considered a causal relationship between the exposure of immune trait and the outcome of gastrointestinal tract cancer, when the *p*-value derived from the IVW method was smaller than 0.05 and the odds ratio (OR) estimates obtained from other MR methods such as MR Egger, Weighted Median, Simple Mode, and Weighted Mode were greater or smaller than 1 or 0, respectively.

3 Results

3.1 Exploration of the causal effect of immune traits on esophagus cancer

A total of 26 immune traits were found to have a significant causal relationship with the occurrence of esophageal cancer. According to the MR analysis based on the IVW method, 14 immune traits were determined to have a protective effect against the onset of esophageal cancer, while the remaining 12 immune traits were identified as risk factors of esophageal cancer (Figure 2). The immune traits with *p*-values less than 0.05 obtained by the IVW method are shown in Supplementary Figure 1A. The top three immune traits with the smallest OR values among the protective factors against esophageal cancer were "CD20 on IgD- CD27-" (IVW p=0.003; OR=0.742, 95%CI [0.609-0.904]), "CCR2 on plasmacytoid DC" (IVW p<0.001; OR=0.761, 95%CI [0.664-0.871]), and "CCR2 on CD62L+ plasmacytoid DC" (IVW p<0.001; OR=0.764, 95%CI [0.666-0.876]). The IVW and MR Egger tests were employed to assess the heterogeneity in the identified protective factors. The Q *p*-values of the three protective factors obtained from the IVW heterogeneity test were 0.582, 0.940, and 0.838, respectively, while the Q *p*-values obtained from the MR Egger test were 0.781, 0.922, and 0.817 (Supplementary Figure 2A).

On the other hand, the top three immune traits with the largest OR values among the risk factors for esophageal cancer were "CD86+ plasmacytoid DC %DC" (IVW p =0.039; OR=1.198, 95%CI [1.009-1.422]), "CD38 on PB/PC" (IVW p =0.047; OR=1.220, 95%CI [1.003-1.483]), and "CD86+ plasmacytoid DC AC" (IVW p =0.036; OR=1.260, 95%CI [1.015-1.563]). The Q *p*-values of these three risk factors obtained from the IVW heterogeneity test were 0.604, 0.566, and 0.200, respectively, while the Q *p*-values obtained from the MR Egger test were 0.630, 0.489, and 0.175 (Supplementary Figure 2A).

Furthermore, there was no substantial pleiotropy observed, as indicated by the Egger intercept (Supplementary Figure 2B). In leave-one-out analyses, altering a single SNP did not alter the direction of the results (Supplementary Figure 2C).

Worth noting is that there exist two protective variables, namely, the "CCR2 on plasmacytoid DC" and "CCR2 on CD62L+ plasmacytoid DC". Albeit having yielded non-significant *p* values under the "Simple mode" analytical approach, all other MR analytical techniques have produced *p* values of less than 0.05, suggestive of significant calculated results of the aforementioned protective factors (Figure 2).

3.2 Exploration of the causal effect of immune traits on stomach cancer

In totality, 29 immune traits were detected to exhibit a significant causal relationship with gastric cancer. Upon conducting MR analysis using the IVW approach, it was determined that 16 immune traits serve a protective role in gastric cancer incidence, whereas the remaining 13 immune traits were identified as risk factors for gastric cancer (refer to Figure 3). The immune traits with *p*-values less than 0.05 obtained by the IVW method are shown in Supplementary Figure 1B. Referring to the 16 identified protective factors, the three immune traits with the smallest odds ratios, denoted as "CD8br and CD8dim % leukocyte" (IVW p=0.004; OR=0.766, 95%CI [0.651 ~ 0.926]), "CD4+ CD8dim %leukocyte" (IVW p=0.043; OR=0.794, 95%CI [0.635 ~ 0.993]), and "CD4+ CD8dim %lymphocyte" (IVW p=0.020; OR=0.828, 95%CI [0.706 ~ 0.971]), were assessed for heterogeneity through the application of both IVW and MR Egger tests. The IVW heterogeneity tests produced Q *p*-values of 0.804, 0.030, and 0.086, and the MR Egger heterogeneity tests yielded values of 0.740, 0.020, and 0.064, respectively (Supplementary Figure 3A).

Of the identified immune traits contributing to gastric cancer risk, the three exhibiting the highest OR were "CD45 on CD4+" (IVW p <0.001; OR=1.394, 95%CI [1.154 ~ 1.683]), "CD28+ DN (CD4-CD8-) AC" (IVW p =0.010; OR=1.296, 95%CI [1.063 ~ 1.581]), and "TD DN (CD4-CD8-) AC" (IVW p =0.002; OR=1.208, 95%CI [1.071 ~ 1.362]). The assessment of heterogeneity of these three identified risk factors through the utilization of IVW tests resulted in Q *p* values of 0.242, 0.522, and 0.404, while the MR Egger tests yielded values of 0.183, 0.690, and 0.353, respectively (Supplementary Figure 3A). Furthermore, no significant pleiotropy was observed as illustrated by the Egger intercept (Supplementary Figure 3B) and the leave-one-out analysis demonstrated that the results were not influenced by the inclusion of any single SNP (Supplementary Figure 3C).

3.3 Exploration of the causal effect of immune traits on cancer of small intestine

Utilizing MR analysis, a total of 29 immune traits were identified to have significant causal relationships with small intestine cancer, with the majority being risk factors, while only 7 immune traits were identified to exhibit protective properties (Figure 4). The immune traits with *p*-values less than 0.05 obtained by the IVW method are shown in Supplementary Figure 1C. The immune traits exhibiting the three smallest ORs as protective factors were "CD27 on IgD- CD38br" (IVW p=0.044; OR=0.732, 95%CI [0.541 ~ 0.992]), "CD8 on CD28- CD8br" (IVW p=0.029; OR=0.775, 95%CI [0.616 ~ 0.973]), and "NK AC" (IVW p=0.028; OR=0.806, 95%CI [0.666 ~ 0.977]). The heterogeneity of the aforementioned protective factors were evaluated through the employment of IVW and MR Egger tests, resulting in Q *p* values of 0.331, 0.898, and 0.499 and 0.594, 0.863, and 0.451, respectively (Supplementary Figure 4A). Within the remaining immune traits

exposure	nsnp	method	pval	OR(95% CI)
Activated Treg AC	15	MR Egger	0.128	1.146 (0.972 to 1.350)
	15	Weighted median	**0.040**	1.183 (1.008 to 1.388)
	15	Inverse variance weighted	**0.034**	1.148 (1.011 to 1.303)
	15	Simple mode	0.346	1.151 (0.868 to 1.527)
	15	Weighted mode	**0.034**	1.184 (1.028 to 1.364)
CCR2 on CD62L+ plasmacytoid DC	18	MR Egger	**0.048**	0.804 (0.658 to 0.982)
	18	Weighted median	**0.009**	0.779 (0.645 to 0.940)
	18	Inverse variance weighted	**<0.001**	0.764 (0.666 to 0.876)
	18	Simple mode	0.196	0.818 (0.615 to 1.089)
	18	Weighted mode	**0.010**	0.771 (0.647 to 0.918)
CCR2 on plasmacytoid DC	18	MR Egger	**0.033**	0.789 (0.646 to 0.963)
	18	Weighted median	**0.010**	0.778 (0.644 to 0.942)
	18	Inverse variance weighted	**<0.001**	0.761 (0.664 to 0.871)
	18	Simple mode	0.200	0.819 (0.611 to 1.098)
	18	Weighted mode	**0.010**	0.772 (0.647 to 0.921)
CD11c on CD62L+ myeloid DC	25	MR Egger	0.428	1.059 (0.921 to 1.218)
	25	Weighted median	0.251	1.097 (0.937 to 1.283)
	25	Inverse variance weighted	**0.019**	1.135 (1.021 to 1.261)
	25	Simple mode	0.343	1.149 (0.868 to 1.521)
	25	Weighted mode	0.228	1.085 (0.954 to 1.234)
CD19 on IgD+ CD38−	30	MR Egger	**0.002**	0.849 (0.772 to 0.932)
	30	Weighted median	**0.013**	0.871 (0.782 to 0.971)
	30	Inverse variance weighted	**0.006**	0.896 (0.829 to 0.968)
	30	Simple mode	0.692	0.952 (0.747 to 1.213)
	30	Weighted mode	**0.011**	0.871 (0.789 to 0.962)
CD20 on IgD− CD27−	18	MR Egger	**0.008**	0.492 (0.311 to 0.780)
	18	Weighted median	**0.018**	0.715 (0.542 to 0.944)
	18	Inverse variance weighted	**0.003**	0.742 (0.609 to 0.904)
	18	Simple mode	0.237	0.727 (0.437 to 1.210)
	18	Weighted mode	0.079	0.685 (0.461 to 1.019)
CD20 on IgD− CD38br	14	MR Egger	**0.018**	0.846 (0.751 to 0.953)
	14	Weighted median	0.069	0.878 (0.763 to 1.010)
	14	Inverse variance weighted	**0.038**	0.898 (0.811 to 0.994)
	14	Simple mode	0.878	0.977 (0.727 to 1.313)
	14	Weighted mode	0.063	0.877 (0.772 to 0.995)
CD25 on activated & secreting Treg	20	MR Egger	**0.028**	1.127 (1.022 to 1.244)
	20	Weighted median	0.126	1.098 (0.974 to 1.239)
	20	Inverse variance weighted	**0.039**	1.091 (1.005 to 1.185)
	20	Simple mode	0.683	1.042 (0.859 to 1.263)
	20	Weighted mode	**0.049**	1.104 (1.007 to 1.210)
CD25 on IgD+ CD38dim	21	MR Egger	0.147	1.107 (0.970 to 1.264)
	21	Weighted median	0.070	1.145 (0.989 to 1.326)
	21	Inverse variance weighted	**0.035**	1.117 (1.008 to 1.237)
	21	Simple mode	0.487	1.095 (0.852 to 1.407)
	21	Weighted mode	0.053	1.149 (1.006 to 1.313)
CD28 on CD39+ activated Treg	18	MR Egger	0.158	1.119 (0.964 to 1.297)
	18	Weighted median	0.136	1.135 (0.961 to 1.340)
	18	Inverse variance weighted	**0.033**	1.124 (1.010 to 1.251)
	18	Simple mode	0.986	1.094 (0.810 to 1.477)
	18	Weighted mode	0.151	1.185 (0.950 to 1.479)
CD28 on secreting Treg	15	MR Egger	0.239	0.927 (0.821 to 1.046)
	15	Weighted median	0.538	0.959 (0.838 to 1.097)
	15	Inverse variance weighted	**0.020**	0.886 (0.800 to 0.981)
	15	Simple mode	0.213	0.843 (0.652 to 1.090)
	15	Weighted mode	0.403	0.943 (0.825 to 1.078)
CD28+ CD45RA+ CD8br %T cell	87	MR Egger	0.056	0.981 (0.962 to 1.000)
	87	Weighted median	**0.039**	0.975 (0.952 to 0.999)
	87	Inverse variance weighted	**0.035**	0.983 (0.968 to 0.999)
	87	Simple mode	**0.042**	0.964 (0.931 to 0.998)
	87	Weighted mode	0.135	0.979 (0.952 to 1.006)
CD3 on activated & secreting Treg	20	MR Egger	0.447	0.929 (0.772 to 1.118)
	20	Weighted median	0.169	0.894 (0.762 to 1.049)
	20	Inverse variance weighted	**0.009**	0.855 (0.760 to 0.961)
	20	Simple mode	0.262	0.873 (0.694 to 1.099)
	20	Weighted mode	0.116	0.878 (0.752 to 1.025)
CD3 on secreting Treg	20	MR Egger	0.181	0.869 (0.714 to 1.059)
	20	Weighted median	0.196	0.900 (0.767 to 1.056)
	20	Inverse variance weighted	**0.044**	0.883 (0.782 to 0.997)
	20	Simple mode	0.154	0.857 (0.699 to 1.051)
	20	Weighted mode	0.138	0.891 (0.769 to 1.031)
CD34 on HSC	12	MR Egger	0.245	0.922 (0.811 to 1.049)
	12	Weighted median	0.131	0.907 (0.799 to 1.030)
	12	Inverse variance weighted	**0.005**	0.878 (0.802 to 0.962)
	12	Simple mode	0.490	0.918 (0.727 to 1.160)
	12	Weighted mode	0.110	0.905 (0.809 to 1.013)
CD38 on PB/PC	15	MR Egger	0.207	1.245 (0.901 to 1.721)
	15	Weighted median	0.268	1.162 (0.891 to 1.516)
	15	Inverse variance weighted	**0.047**	1.220 (1.003 to 1.483)
	15	Simple mode	0.544	1.138 (0.757 to 1.709)
	15	Weighted mode	0.237	1.190 (0.903 to 1.569)
CD39+ resting Treg % CD4 Treg	35	MR Egger	0.162	1.059 (0.979 to 1.147)
	35	Weighted median	0.518	1.028 (0.945 to 1.118)
	35	Inverse variance weighted	0.050	1.064 (1.000 to 1.132)
	35	Simple mode	0.418	1.071 (0.909 to 1.261)
	35	Weighted mode	0.392	1.030 (0.964 to 1.100)
CD45 on lymphocyte	24	MR Egger	0.264	1.140 (0.911 to 1.428)
	24	Weighted median	0.148	1.178 (0.943 to 1.470)
	24	Inverse variance weighted	**0.022**	1.192 (1.026 to 1.386)
	24	Simple mode	0.335	1.196 (0.836 to 1.707)
	24	Weighted mode	0.125	1.196 (0.952 to 1.490)
CD45RA− CD28− CD8br %CD8br	49	MR Egger	**0.046**	1.003 (1.000 to 1.007)
	49	Weighted median	0.363	1.002 (0.998 to 1.006)
	49	Inverse variance weighted	**0.035**	1.003 (1.000 to 1.006)
	49	Simple mode	0.172	1.004 (0.998 to 1.010)
	49	Weighted mode	0.325	1.002 (0.998 to 1.005)
CD86+ plasmacytoid DC %DC	26	MR Egger	0.848	1.030 (0.761 to 1.394)
	26	Weighted median	0.373	1.135 (0.859 to 1.498)
	26	Inverse variance weighted	**0.039**	1.198 (1.009 to 1.422)
	26	Simple mode	0.547	1.159 (0.721 to 1.863)
	26	Weighted mode	0.568	1.111 (0.778 to 1.586)
CD86+ plasmacytoid DC AC	20	MR Egger	0.099	1.381 (0.960 to 1.987)
	20	Weighted median	0.241	1.188 (0.890 to 1.586)
	20	Inverse variance weighted	**0.036**	1.260 (1.015 to 1.563)
	20	Simple mode	**0.045**	1.771 (1.009 to 2.988)
	20	Weighted mode	0.155	1.252 (0.930 to 1.686)
CM DN (CD4−CD8−) AC	4	MR Egger	0.351	0.860 (0.673 to 1.099)
	4	Weighted median	0.086	0.846 (0.699 to 1.024)
	4	Inverse variance weighted	**0.034**	0.842 (0.718 to 0.987)
	4	Simple mode	0.322	0.856 (0.661 to 1.108)
	4	Weighted mode	0.161	0.846 (0.709 to 1.010)
FSC−A on B cell	19	MR Egger	0.417	0.877 (0.642 to 1.196)
	19	Weighted median	**0.028**	0.760 (0.595 to 0.971)
	19	Inverse variance weighted	**0.041**	0.838 (0.707 to 0.993)
	19	Simple mode	0.234	0.786 (0.535 to 1.153)
	19	Weighted mode	0.068	0.776 (0.601 to 1.003)
Granulocyte %leukocyte	25	MR Egger	0.646	0.953 (0.778 to 1.167)
	25	Weighted median	0.121	0.846 (0.685 to 1.045)
	25	Inverse variance weighted	**0.014**	0.832 (0.719 to 0.963)
	25	Simple mode	0.262	0.817 (0.578 to 1.154)
	25	Weighted mode	0.099	0.830 (0.671 to 1.027)
Myeloid DC %DC	26	MR Egger	0.196	0.832 (0.635 to 1.091)
	26	Weighted median	0.179	0.858 (0.687 to 1.073)
	26	Inverse variance weighted	**0.014**	0.820 (0.699 to 0.961)
	26	Simple mode	0.237	0.798 (0.553 to 1.150)
	26	Weighted mode	0.153	0.850 (0.685 to 1.055)
TD CD4+ %T cell	25	MR Egger	**0.017**	1.165 (1.037 to 1.308)
	25	Weighted median	**0.018**	1.174 (1.027 to 1.342)
	25	Inverse variance weighted	**0.003**	1.160 (1.053 to 1.278)
	25	Simple mode	0.092	1.249 (0.974 to 1.600)
	25	Weighted mode	**0.009**	1.170 (1.050 to 1.303)

0 1 2

FIGURE 2
Forest plot for MR analysis with esophagus cancer as the outcome.

exposure	nsnp	method	pval	OR(95% CI)
B cell AC	29	MR Egger	0.468	0.929 (0.764 to 1.130)
	29	Weighted median	0.188	0.899 (0.768 to 1.053)
	29	Inverse variance weighted	**0.044**	0.894 (0.802 to 0.997)
	29	Simple mode	0.797	0.963 (0.726 to 1.279)
	29	Weighted mode	0.498	0.933 (0.766 to 1.137)
CCR2 on CD14− CD16+ monocyte	27	MR Egger	0.082	1.079 (0.994 to 1.171)
	27	Weighted median	0.267	1.051 (0.963 to 1.148)
	27	Inverse variance weighted	**0.043**	1.071 (1.002 to 1.144)
	27	Simple mode	0.262	1.084 (0.945 to 1.243)
	27	Weighted mode	0.099	1.063 (0.991 to 1.140)
CCR2 on CD14+ CD16+ monocyte	36	MR Egger	0.050	1.061 (1.002 to 1.124)
	36	Weighted median	0.178	1.050 (0.978 to 1.128)
	36	Inverse variance weighted	**0.019**	1.058 (1.010 to 1.110)
	36	Simple mode	0.198	1.076 (0.965 to 1.200)
	36	Weighted mode	0.184	1.044 (0.981 to 1.110)
CD11b on CD66b++ myeloid cell	17	MR Egger	0.895	1.052 (0.819 to 1.351)
	17	Weighted median	**0.041**	1.170 (1.007 to 1.361)
	17	Inverse variance weighted	**0.035**	1.142 (1.009 to 1.292)
	17	Simple mode	0.142	1.229 (0.946 to 1.597)
	17	Weighted mode	0.471	1.086 (0.873 to 1.351)
CD11c+ HLA DR++ monocyte AC	17	MR Egger	0.450	1.087 (0.880 to 1.342)
	17	Weighted median	0.097	1.168 (0.972 to 1.404)
	17	Inverse variance weighted	**0.023**	1.170 (1.022 to 1.340)
	17	Simple mode	0.105	1.286 (0.965 to 1.714)
	17	Weighted mode	0.128	1.174 (0.965 to 1.429)
CD19 on B cell	22	MR Egger	0.151	0.885 (0.753 to 1.039)
	22	Weighted median	0.229	0.908 (0.776 to 1.062)
	22	Inverse variance weighted	**0.038**	0.893 (0.802 to 0.993)
	22	Simple mode	0.116	0.805 (0.621 to 1.043)
	22	Weighted mode	0.178	0.892 (0.759 to 1.048)
CD25hi %CD4+	25	MR Egger	0.062	0.868 (0.754 to 1.000)
	25	Weighted median	**0.035**	0.857 (0.742 to 0.989)
	25	Inverse variance weighted	**0.044**	0.907 (0.825 to 0.997)
	25	Simple mode	0.320	0.890 (0.711 to 1.114)
	25	Weighted mode	**0.048**	0.871 (0.765 to 0.992)
CD28− DN (CD4−CD8−) %T cell	22	MR Egger	0.077	1.150 (0.993 to 1.333)
	22	Weighted median	0.072	1.146 (0.988 to 1.329)
	22	Inverse variance weighted	**0.015**	1.129 (1.023 to 1.246)
	22	Simple mode	0.099	1.257 (0.970 to 1.631)
	22	Weighted mode	**0.023**	1.189 (1.035 to 1.365)
CD28−DN(CD4−CD8−)%Tcell	22	MR Egger	0.077	1.150 (0.993 to 1.333)
	22	Weighted median	0.078	1.146 (0.985 to 1.333)
	22	Inverse variance weighted	**0.015**	1.129 (1.023 to 1.246)
	22	Simple mode	0.124	1.257 (0.951 to 1.663)
	22	Weighted mode	**0.026**	1.189 (1.031 to 1.370)
CD28 on CD39+ activated Treg	18	MR Egger	0.300	1.058 (0.954 to 1.174)
	18	Weighted median	0.138	1.084 (0.975 to 1.205)
	18	Inverse variance weighted	**0.006**	1.111 (1.031 to 1.197)
	18	Simple mode	0.247	1.098 (0.942 to 1.279)
	18	Weighted mode	0.153	1.083 (0.975 to 1.203)
CD28+ DN (CD4−CD8−) AC	10	MR Egger	0.760	1.054 (0.762 to 1.458)
	10	Weighted median	0.246	1.171 (0.897 to 1.529)
	10	Inverse variance weighted	**0.010**	1.296 (1.063 to 1.581)
	10	Simple mode	0.626	1.127 (0.706 to 1.794)
	10	Weighted mode	0.446	1.138 (0.828 to 1.562)
CD3 on CD28− CD8br	20	MR Egger	0.447	0.896 (0.679 to 1.182)
	20	Weighted median	0.156	0.892 (0.761 to 1.045)
	20	Inverse variance weighted	**0.019**	0.871 (0.776 to 0.977)
	20	Simple mode	0.393	0.884 (0.670 to 1.166)
	20	Weighted mode	0.437	0.917 (0.742 to 1.135)
CD39 on CD39+ activated Treg	22	MR Egger	0.170	0.864 (0.706 to 1.057)
	22	Weighted median	0.209	0.922 (0.813 to 1.046)
	22	Inverse variance weighted	**0.035**	0.907 (0.829 to 0.993)
	22	Simple mode	0.435	0.931 (0.782 to 1.110)
	22	Weighted mode	0.180	0.915 (0.808 to 1.037)
CD39+ CD4+ %CD4+	25	MR Egger	0.516	0.972 (0.895 to 1.057)
	25	Weighted median	0.503	0.972 (0.894 to 1.057)
	25	Inverse variance weighted	**0.027**	0.932 (0.876 to 0.992)
	25	Simple mode	0.110	0.872 (0.743 to 1.025)
	25	Weighted mode	0.207	0.951 (0.881 to 1.026)
CD4 on CD39+ resting Treg	13	MR Egger	0.281	0.925 (0.808 to 1.059)
	13	Weighted median	0.162	0.908 (0.793 to 1.040)
	13	Inverse variance weighted	**0.026**	0.893 (0.808 to 0.986)
	13	Simple mode	0.205	0.874 (0.718 to 1.064)
	13	Weighted mode	0.225	0.920 (0.811 to 1.045)
CD4+ CD8dim %leukocyte	13	MR Egger	0.460	0.816 (0.486 to 1.372)
	13	Weighted median	**0.038**	0.789 (0.631 to 0.986)
	13	Inverse variance weighted	**0.043**	0.794 (0.635 to 0.993)
	13	Simple mode	0.064	0.594 (0.361 to 0.979)
	13	Weighted mode	0.111	0.792 (0.606 to 1.033)
CD4+ CD8dim %lymphocyte	18	MR Egger	0.210	0.816 (0.602 to 1.107)
	18	Weighted median	0.073	0.837 (0.688 to 1.017)
	18	Inverse variance weighted	**0.020**	0.828 (0.706 to 0.971)
	18	Simple mode	**0.029**	0.640 (0.443 to 0.923)
	18	Weighted mode	0.178	0.859 (0.696 to 1.061)
CD45 on CD33br HLA DR+	16	MR Egger	0.058	0.917 (0.846 to 0.996)
	16	Weighted median	0.176	0.939 (0.856 to 1.029)
	16	Inverse variance weighted	**0.014**	0.923 (0.866 to 0.984)
	16	Simple mode	0.950	0.995 (0.859 to 1.153)
	16	Weighted mode	0.116	0.936 (0.866 to 1.012)
CD45 on CD4+	13	MR Egger	0.209	1.383 (0.859 to 2.225)
	13	Weighted median	**0.009**	1.405 (1.088 to 1.816)
	13	Inverse variance weighted	**<0.001**	1.394 (1.154 to 1.683)
	13	Simple mode	**0.041**	1.651 (1.074 to 2.536)
	13	Weighted mode	0.053	1.658 (1.045 to 2.631)
CD62L− HLA DR++ monocyte AC	19	MR Egger	0.912	1.022 (0.703 to 1.484)
	19	Weighted median	0.106	1.191 (0.963 to 1.473)
	19	Inverse variance weighted	**0.045**	1.168 (1.003 to 1.360)
	19	Simple mode	0.302	1.188 (0.865 to 1.632)
	19	Weighted mode	0.214	1.201 (0.909 to 1.587)
CD8br and CD8dim %leukocyte	14	MR Egger	0.261	0.756 (0.476 to 1.202)
	14	Weighted median	**0.007**	0.715 (0.560 to 0.913)
	14	Inverse variance weighted	**0.005**	0.776 (0.651 to 0.926)
	14	Simple mode	0.057	0.633 (0.412 to 0.972)
	14	Weighted mode	**0.036**	0.639 (0.439 to 0.931)
HLA DR on CD33br HLA DR+ CD14dim	20	MR Egger	0.518	1.044 (0.919 to 1.186)
	20	Weighted median	0.213	1.067 (0.964 to 1.181)
	20	Inverse variance weighted	**0.030**	1.087 (1.008 to 1.171)
	20	Simple mode	0.302	1.091 (0.929 to 1.283)
	20	Weighted mode	0.291	1.064 (0.951 to 1.191)
HLA DR+ T cell%lymphocyte	24	MR Egger	0.143	1.080 (0.979 to 1.192)
	24	Weighted median	**0.048**	1.098 (1.001 to 1.205)
	24	Inverse variance weighted	**0.004**	1.107 (1.033 to 1.186)
	24	Simple mode	0.101	1.148 (0.980 to 1.344)
	24	Weighted mode	0.141	1.077 (0.979 to 1.186)
HVEM on naive CD4+	16	MR Egger	0.362	0.942 (0.833 to 1.066)
	16	Weighted median	0.263	0.935 (0.831 to 1.052)
	16	Inverse variance weighted	**0.039**	0.922 (0.854 to 0.996)
	16	Simple mode	0.165	0.879 (0.739 to 1.045)
	16	Weighted mode	0.284	0.933 (0.826 to 1.054)
IgD on IgD+ CD38−	25	MR Egger	0.284	0.928 (0.811 to 1.061)
	25	Weighted median	0.084	0.903 (0.805 to 1.014)
	25	Inverse variance weighted	**0.021**	0.903 (0.829 to 0.985)
	25	Simple mode	0.527	0.929 (0.743 to 1.162)
	25	Weighted mode	0.095	0.915 (0.828 to 1.012)
Resting Treg AC	25	MR Egger	0.651	1.036 (0.892 to 1.203)
	25	Weighted median	0.553	1.042 (0.911 to 1.191)
	25	Inverse variance weighted	**0.044**	1.098 (1.002 to 1.203)
	25	Simple mode	0.351	1.089 (0.903 to 1.315)
	25	Weighted mode	0.366	1.062 (0.934 to 1.208)
SSC−A on HLA DR+ NK	27	MR Egger	0.061	0.913 (0.834 to 1.000)
	27	Weighted median	0.325	0.951 (0.860 to 1.051)
	27	Inverse variance weighted	**0.016**	0.919 (0.859 to 0.985)
	27	Simple mode	0.489	0.946 (0.809 to 1.106)
	27	Weighted mode	0.191	0.938 (0.854 to 1.030)
T cell %lymphocyte	17	MR Egger	0.104	0.676 (0.434 to 1.052)
	17	Weighted median	0.190	0.878 (0.722 to 1.067)
	17	Inverse variance weighted	**0.049**	0.866 (0.750 to 1.000)
	17	Simple mode	0.350	0.871 (0.658 to 1.153)
	17	Weighted mode	0.261	0.855 (0.657 to 1.113)
TD DN (CD4−CD8−) AC	20	MR Egger	0.131	1.171 (0.963 to 1.423)
	20	Weighted median	0.091	1.179 (0.974 to 1.426)
	20	Inverse variance weighted	**0.002**	1.208 (1.071 to 1.362)
	20	Simple mode	0.244	1.193 (0.895 to 1.591)
	20	Weighted mode	0.121	1.156 (0.970 to 1.378)

0 1

FIGURE 3
Forest plot for MR analysis with stomach cancer as the outcome.

10.3389/fimmu.2024.1343512

FIGURE 4
Forest plot for MR analysis with cancer of small intestine as the outcome.

associated with risk, the three with the highest ORs were "CD24 on IgD- CD38dim" (IVW p =0.024; OR=1.497, 95%CI [1.054 ~ 2.126]), "CD28- CD8br %T cell" (IVW p =0.039; OR=1.302, 95% CI [1.013 ~ 1.673]), and "CD4 on CD39+ CD4+" (IVW p =0.002; OR=1.270, 95%CI[1.094 ~ 1.474]). The heterogeneity of these three identified risk factors were assessed through IVW testing, resulting in Q *p* values of 0.908, 0.997, and 0.585, while the MR Egger test yielded values of 0.922, 0.995, and 0.686, respectively (Supplementary Figure 4A). Furthermore, no significant pleiotropy was observed, as demonstrated by the Egger intercept (Supplementary Figure 4B) and the results were not influenced by the inclusion of any single SNP, as demonstrated by the leave-one-out analysis (Supplementary Figure 4C).

3.4 Exploration of the causal effect of immune traits on colon cancer

A total of 26 immune traits have been identified to exhibit significant causal relationships with colon cancer, with 12 being risk factors and 14 being protective factors (Figure 5). The immune traits with *p*-values less than 0.05 obtained by the IVW method are shown in Supplementary Figure 1D. The top 3 immune traits with the smallest ORs as protective factors were "CD62L- HLA DR++ monocyte %monocyte" (IVW p=0.039; OR=0.893, 95%CI [0.603 ~ 0.994]), "CD8 on CM CD8br" (IVW p=0.011; OR=0.897, 95%CI [0.825 ~ 0.976]), and "CD4 on TD CD4+" (IVW p=0.004; OR=0.920, 95%CI [0.870 ~ 0.973]). The heterogeneity of the aforementioned protective factors were evaluated through the employment of IVW and MR Egger tests, resulting in Q *p* values of 0.882 (IVW), 0.892 (IVW), and 0.429 (IVW), and 0.824 (Egger), 0.842 (Egger), and 0.378 (Egger), respectively (Supplementary Figure 5A). Within the immune traits associated with colon cancer risk, the three with the highest ORs were "CD45 on CD4 +" (IVW p=0.043; OR=1.107, 95%CI [1.003 ~ 1.221]), "EM DN (CD4-CD8-) %T cell" (IVW p=0.003; OR=1.100, 95%CI [1.032 ~ 1.172]), and "HLA DR++ monocyte %leukocyte" (IVW p=0.048; OR=1.093, 95%CI [1.001 ~ 1.194]). The heterogeneity of these three identified risk factors were assessed through IVW testing, resulting in Q *p* values of 0.879, 0.598, and 0.628, while the MR Egger test yielded values of 0.826, 0.539, and 0.522, respectively (Supplementary Figure 5A). Additionally, the Egger intercept was not significant, as indicated in Supplementary Figure 4B, and the leave-one-out analysis suggested that the results were not influenced by any single SNP (Supplementary Figure 5C).

3.5 Exploration of the causal effect of immune traits on rectal cancer

A significant causal relationship between 28 immune traits and rectal cancer has been discovered, with 19 identified as risk factors and only 9 as protective factors (Figure 6). The immune traits with *p*-values less than 0.05 obtained by the IVW method are shown in Supplementary Figure 1D. The top three protective factors with the smallest ORs were identified as "CD64 on CD14+ CD16+

10.3389/fimmu.2024.1343512

exposure	nsnp	method	pval	OR(95% CI)
BAFF−R on CD20−	13	MR Egger	**0.019**	0.869 (0.785 to 0.961)
	13	Weighted median	0.052	0.910 (0.828 to 1.001)
	13	Inverse variance weighted	**0.044**	0.928 (0.862 to 0.998)
	13	Simple mode	0.686	0.964 (0.812 to 1.145)
	13	Weighted mode	0.089	0.921 (0.843 to 1.005)
CD16−CD56 on NK	28	MR Egger	0.134	1.081 (0.979 to 1.194)
	28	Weighted median	0.069	1.062 (0.995 to 1.133)
	28	Inverse variance weighted	**0.039**	1.052 (1.002 to 1.105)
	28	Simple mode	0.247	1.059 (0.963 to 1.165)
	28	Weighted mode	0.124	1.062 (0.986 to 1.145)
CD19 on IgD+ CD38− naive	19	MR Egger	0.268	0.980 (0.948 to 1.014)
	19	Weighted median	0.202	0.977 (0.943 to 1.013)
	19	Inverse variance weighted	**0.028**	0.968 (0.940 to 0.996)
	19	Simple mode	0.524	0.967 (0.875 to 1.069)
	19	Weighted mode	0.167	0.978 (0.949 to 1.008)
CD19 on IgD+ CD38−	30	MR Egger	0.427	0.985 (0.949 to 1.022)
	30	Weighted median	0.206	0.974 (0.934 to 1.015)
	30	Inverse variance weighted	**0.030**	0.965 (0.935 to 0.997)
	30	Simple mode	0.830	0.990 (0.906 to 1.082)
	30	Weighted mode	0.124	0.972 (0.939 to 1.007)
CD25 on CD4+	15	MR Egger	0.160	1.032 (0.990 to 1.075)
	15	Weighted median	0.157	1.032 (0.988 to 1.079)
	15	Inverse variance weighted	**0.034**	1.037 (1.003 to 1.073)
	15	Simple mode	0.204	1.070 (0.969 to 1.181)
	15	Weighted mode	0.105	1.032 (0.996 to 1.068)
CD25 on IgD− CD24−	25	MR Egger	0.840	1.014 (0.884 to 1.165)
	25	Weighted median	0.133	1.084 (0.976 to 1.204)
	25	Inverse variance weighted	**0.036**	1.085 (1.005 to 1.170)
	25	Simple mode	0.587	1.051 (0.880 to 1.256)
	25	Weighted mode	0.340	1.068 (0.935 to 1.219)
CD25 on IgD− CD38−	21	MR Egger	0.059	0.945 (0.894 to 0.999)
	21	Weighted median	0.053	0.944 (0.890 to 1.001)
	21	Inverse variance weighted	**0.012**	0.947 (0.908 to 0.988)
	21	Simple mode	0.166	0.932 (0.846 to 1.026)
	21	Weighted mode	0.052	0.947 (0.900 to 0.997)
CD25 on IgD+ CD24+	26	MR Egger	0.053	0.963 (0.929 to 0.999)
	26	Weighted median	0.089	0.963 (0.922 to 1.006)
	26	Inverse variance weighted	**0.017**	0.964 (0.936 to 0.994)
	26	Simple mode	0.407	0.960 (0.874 to 1.055)
	26	Weighted mode	0.090	0.966 (0.929 to 1.004)
CD25 on IgD+ CD38−	27	MR Egger	**0.041**	0.966 (0.935 to 0.997)
	27	Weighted median	0.099	0.966 (0.926 to 1.007)
	27	Inverse variance weighted	**0.006**	0.963 (0.937 to 0.989)
	27	Simple mode	**0.001**	0.834 (0.755 to 0.921)
	27	Weighted mode	0.074	0.969 (0.938 to 1.002)
CD25hi CD45RA− CD4 not Treg %T cell	28	MR Egger	0.566	0.989 (0.951 to 1.028)
	28	Weighted median	0.190	0.971 (0.929 to 1.015)
	28	Inverse variance weighted	**0.049**	0.969 (0.940 to 1.000)
	28	Simple mode	0.466	0.973 (0.905 to 1.046)
	28	Weighted mode	0.183	0.976 (0.942 to 1.011)
CD25hi CD45RA+ CD4 not Treg AC	25	MR Egger	0.344	0.972 (0.916 to 1.030)
	25	Weighted median	0.277	0.967 (0.910 to 1.027)
	25	Inverse variance weighted	**0.033**	0.955 (0.915 to 0.996)
	25	Simple mode	0.542	0.971 (0.886 to 1.065)
	25	Weighted mode	0.259	0.966 (0.910 to 1.025)
CD28+ CD45RA+ CD8dim %T cell	37	MR Egger	**0.023**	1.020 (1.004 to 1.037)
	37	Weighted median	0.139	1.016 (0.995 to 1.038)
	37	Inverse variance weighted	**0.042**	1.015 (1.001 to 1.031)
	37	Simple mode	0.463	1.014 (0.978 to 1.052)
	37	Weighted mode	**0.038**	1.019 (1.002 to 1.037)
CD3 on HLA DR+ CD8br	25	MR Egger	**0.017**	1.118 (1.027 to 1.218)
	25	Weighted median	0.074	1.074 (0.993 to 1.162)
	25	Inverse variance weighted	0.050	1.054 (1.000 to 1.112)
	25	Simple mode	0.383	1.062 (0.930 to 1.211)
	25	Weighted mode	0.078	1.080 (0.995 to 1.172)
CD33 on CD33dim HLA DR+ CD11b−	21	MR Egger	0.401	0.975 (0.920 to 1.033)
	21	Weighted median	0.295	0.979 (0.940 to 1.019)
	21	Inverse variance weighted	**0.047**	0.965 (0.932 to 1.000)
	21	Simple mode	0.796	0.987 (0.892 to 1.091)
	21	Weighted mode	0.324	0.980 (0.941 to 1.019)
CD39+ resting Treg %resting Treg	27	MR Egger	0.244	1.031 (0.981 to 1.083)
	27	Weighted median	0.109	1.037 (0.992 to 1.084)
	27	Inverse variance weighted	**0.019**	1.042 (1.007 to 1.079)
	27	Simple mode	0.059	1.080 (1.000 to 1.166)
	27	Weighted mode	0.062	1.039 (1.000 to 1.080)
CD4 on TD CD4+	23	MR Egger	0.063	0.906 (0.822 to 1.000)
	23	Weighted median	**0.047**	0.923 (0.852 to 0.999)
	23	Inverse variance weighted	**0.004**	0.820 (0.870 to 0.973)
	23	Simple mode	0.544	0.960 (0.843 to 1.093)
	23	Weighted mode	0.094	0.925 (0.848 to 1.009)
CD45 on CD4+	13	MR Egger	0.485	1.091 (0.861 to 1.382)
	13	Weighted median	0.067	1.132 (0.992 to 1.292)
	13	Inverse variance weighted	**0.043**	1.107 (1.003 to 1.221)
	13	Simple mode	0.207	1.175 (0.927 to 1.489)
	13	Weighted mode	0.166	1.185 (0.946 to 1.485)
CD62L− HLA DR++ monocyte %monocyte	11	MR Egger	0.517	0.910 (0.690 to 1.198)
	11	Weighted median	0.117	0.887 (0.763 to 1.031)
	11	Inverse variance weighted	**0.039**	0.893 (0.803 to 0.994)
	11	Simple mode	0.297	0.883 (0.708 to 1.102)
	11	Weighted mode	0.160	0.857 (0.702 to 1.046)
CD8 on CM CD8br	13	MR Egger	0.379	0.904 (0.728 to 1.122)
	13	Weighted median	0.115	0.913 (0.815 to 1.023)
	13	Inverse variance weighted	**0.011**	0.897 (0.825 to 0.976)
	13	Simple mode	0.117	0.863 (0.728 to 1.024)
	13	Weighted mode	0.475	0.945 (0.812 to 1.099)
EM DN (CD4−CD8−) %T cell	23	MR Egger	0.124	1.091 (0.981 to 1.214)
	23	Weighted median	0.101	1.076 (0.986 to 1.174)
	23	Inverse variance weighted	**0.003**	1.100 (1.032 to 1.172)
	23	Simple mode	0.288	1.074 (0.944 to 1.222)
	23	Weighted mode	0.104	1.086 (0.987 to 1.195)
HLA DR++ monocyte %leukocyte	8	MR Egger	0.476	1.068 (0.901 to 1.266)
	8	Weighted median	0.282	1.071 (0.945 to 1.213)
	8	Inverse variance weighted	**0.048**	1.093 (1.001 to 1.194)
	8	Simple mode	0.806	1.022 (0.857 to 1.203)
	8	Weighted mode	0.526	1.046 (0.917 to 1.193)
HLA DR++ monocyte %monocyte	20	MR Egger	0.197	1.079 (0.966 to 1.205)
	20	Weighted median	0.144	1.064 (0.979 to 1.157)
	20	Inverse variance weighted	**0.015**	1.078 (1.015 to 1.146)
	20	Simple mode	0.120	1.117 (0.978 to 1.275)
	20	Weighted mode	0.104	1.076 (0.989 to 1.170)
IgD+ CD38br %B cell	25	MR Egger	0.110	0.934 (0.862 to 1.012)
	25	Weighted median	0.066	0.933 (0.867 to 1.005)
	25	Inverse variance weighted	**0.026**	0.941 (0.893 to 0.993)
	25	Simple mode	0.164	0.912 (0.804 to 1.034)
	25	Weighted mode	0.056	0.934 (0.874 to 0.998)
Memory B cell %B cell	27	MR Egger	0.504	1.029 (0.948 to 1.116)
	27	Weighted median	0.341	1.038 (0.961 to 1.121)
	27	Inverse variance weighted	**0.038**	1.057 (1.003 to 1.115)
	27	Simple mode	0.811	1.016 (0.894 to 1.155)
	27	Weighted mode	0.346	1.035 (0.965 to 1.111)
Naive−mature B cell %B cell	27	MR Egger	0.425	0.974 (0.915 to 1.036)
	27	Weighted median	0.239	0.963 (0.906 to 1.025)
	27	Inverse variance weighted	**0.022**	0.948 (0.906 to 0.992)
	27	Simple mode	0.748	0.982 (0.883 to 1.093)
	27	Weighted mode	0.241	0.964 (0.908 to 1.024)
PB/PC AC	24	MR Egger	0.293	1.024 (0.981 to 1.068)
	24	Weighted median	0.140	1.036 (0.988 to 1.087)
	24	Inverse variance weighted	**0.027**	1.043 (1.005 to 1.083)
	24	Simple mode	0.397	1.034 (0.958 to 1.117)
	24	Weighted mode	0.194	1.028 (0.987 to 1.071)

FIGURE 5
Forest plot for MR analysis with colon cancer as the outcome.

exposure	nsnp	method	pval	OR(95% CI)
B cell %lymphocyte	32	MR Egger	0.152	1.091 (0.972 to 1.225)
	32	Weighted median	0.108	1.086 (0.982 to 1.201)
	32	Inverse variance weighted	**0.020**	1.083 (1.012 to 1.158)
	32	Simple mode	0.347	1.096 (0.908 to 1.324)
	32	Weighted mode	0.233	1.099 (0.944 to 1.279)
BAFF−R on IgD− CD38−	17	MR Egger	0.399	0.971 (0.909 to 1.038)
	17	Weighted median	0.265	0.966 (0.908 to 1.027)
	17	Inverse variance weighted	**0.007**	0.936 (0.892 to 0.982)
	17	Simple mode	0.083	0.894 (0.794 to 1.007)
	17	Weighted mode	0.124	0.956 (0.906 to 1.009)
BAFF−R on IgD− CD38br	14	MR Egger	0.275	0.893 (0.736 to 1.084)
	14	Weighted median	0.200	0.913 (0.795 to 1.049)
	14	Inverse variance weighted	**0.043**	0.900 (0.813 to 0.997)
	14	Simple mode	0.566	0.935 (0.749 to 1.168)
	14	Weighted mode	0.233	0.914 (0.794 to 1.052)
CCR2 on CD14− CD16+ monocyte	27	MR Egger	0.256	1.031 (0.980 to 1.084)
	27	Weighted median	0.446	1.030 (0.954 to 1.112)
	27	Inverse variance weighted	**0.032**	1.047 (1.004 to 1.092)
	27	Simple mode	0.332	1.062 (0.942 to 1.197)
	27	Weighted mode	0.241	1.039 (0.976 to 1.105)
CD11c+ HLA DR++ monocyte %monocyte	16	MR Egger	0.123	1.063 (0.988 to 1.143)
	16	Weighted median	0.140	1.064 (0.980 to 1.156)
	16	Inverse variance weighted	**0.042**	1.065 (1.002 to 1.131)
	16	Simple mode	0.388	1.093 (0.899 to 1.328)
	16	Weighted mode	0.112	1.063 (0.990 to 1.141)
CD14− CD16+ monocyte AC	17	MR Egger	0.142	0.925 (0.839 to 1.021)
	17	Weighted median	0.057	0.909 (0.824 to 1.003)
	17	Inverse variance weighted	**0.026**	0.917 (0.849 to 0.990)
	17	Simple mode	0.137	0.880 (0.750 to 1.033)
	17	Weighted mode	**0.023**	0.897 (0.824 to 0.976)
CD25 on activated Treg	17	MR Egger	0.057	0.785 (0.623 to 0.988)
	17	Weighted median	0.115	0.875 (0.740 to 1.033)
	17	Inverse variance weighted	**0.005**	0.845 (0.752 to 0.950)
	17	Simple mode	0.534	0.909 (0.677 to 1.221)
	17	Weighted mode	0.380	0.888 (0.686 to 1.149)
CD25 on memory B cell	22	MR Egger	0.110	1.073 (0.988 to 1.166)
	22	Weighted median	0.192	1.062 (0.970 to 1.163)
	22	Inverse variance weighted	**0.012**	1.083 (1.018 to 1.152)
	22	Simple mode	0.227	1.096 (0.949 to 1.266)
	22	Weighted mode	0.112	1.069 (0.988 to 1.157)
CD25hi CD45RA+ CD4 not Treg AC	25	MR Egger	0.170	0.935 (0.851 to 1.028)
	25	Weighted median	0.113	0.937 (0.865 to 1.015)
	25	Inverse variance weighted	**0.034**	0.930 (0.870 to 0.995)
	25	Simple mode	**0.020**	0.841 (0.734 to 0.963)
	25	Weighted mode	**0.043**	0.922 (0.856 to 0.993)
CD27 on IgD+ CD38− unsw mem	23	MR Egger	**0.010**	0.859 (0.773 to 0.954)
	23	Weighted median	0.067	0.924 (0.849 to 1.006)
	23	Inverse variance weighted	**0.011**	0.925 (0.871 to 0.982)
	23	Simple mode	0.209	0.910 (0.789 to 1.050)
	23	Weighted mode	**0.026**	0.898 (0.822 to 0.981)
CD27 on sw mem	30	MR Egger	0.292	0.931 (0.817 to 1.061)
	30	Weighted median	0.152	0.934 (0.850 to 1.026)
	30	Inverse variance weighted	**0.040**	0.935 (0.877 to 0.997)
	30	Simple mode	0.540	0.949 (0.803 to 1.121)
	30	Weighted mode	0.200	0.939 (0.855 to 1.032)
CD27 on unsw mem	30	MR Egger	0.115	0.896 (0.785 to 1.023)
	30	Weighted median	0.102	0.918 (0.829 to 1.017)
	30	Inverse variance weighted	**0.035**	0.931 (0.871 to 0.995)
	30	Simple mode	0.396	0.930 (0.789 to 1.097)
	30	Weighted mode	0.286	0.936 (0.831 to 1.054)
CD28 on CD4 Treg	24	MR Egger	0.199	0.966 (0.917 to 1.017)
	24	Weighted median	0.052	0.945 (0.892 to 1.001)
	24	Inverse variance weighted	**0.016**	0.948 (0.907 to 0.990)
	24	Simple mode	0.359	0.957 (0.872 to 1.050)
	24	Weighted mode	0.089	0.957 (0.911 to 1.005)
CD4+ %leukocyte	13	MR Egger	0.993	1.002 (0.706 to 1.420)
	13	Weighted median	0.282	1.118 (0.913 to 1.369)
	13	Inverse variance weighted	**0.049**	1.160 (1.001 to 1.345)
	13	Simple mode	0.700	1.062 (0.787 to 1.434)
	13	Weighted mode	0.798	1.037 (0.788 to 1.365)
CD4+ AC	23	MR Egger	0.057	0.915 (0.840 to 0.998)
	23	Weighted median	**0.044**	0.895 (0.804 to 0.997)
	23	Inverse variance weighted	**0.004**	0.911 (0.855 to 0.971)
	23	Simple mode	0.143	0.873 (0.733 to 1.040)
	23	Weighted mode	**0.046**	0.904 (0.824 to 0.993)
CD40 on CD14− CD16+ monocyte	26	MR Egger	**0.007**	1.096 (1.031 to 1.165)
	26	Weighted median	0.086	1.065 (0.991 to 1.145)
	26	Inverse variance weighted	**0.011**	1.060 (1.013 to 1.110)
	26	Simple mode	0.507	1.044 (0.922 to 1.182)
	26	Weighted mode	**0.023**	1.074 (1.014 to 1.138)
CD62L− DC %DC	20	MR Egger	**0.019**	0.902 (0.835 to 0.976)
	20	Weighted median	0.504	0.971 (0.892 to 1.058)
	20	Inverse variance weighted	**0.012**	0.928 (0.876 to 0.984)
	20	Simple mode	0.421	0.950 (0.841 to 1.073)
	20	Weighted mode	0.180	0.950 (0.884 to 1.021)
CD62L− myeloid DC %DC	24	MR Egger	**0.041**	0.918 (0.850 to 0.992)
	24	Weighted median	0.106	0.936 (0.864 to 1.014)
	24	Inverse variance weighted	**0.004**	0.923 (0.874 to 0.974)
	24	Simple mode	0.909	0.992 (0.872 to 1.129)
	24	Weighted mode	0.069	0.935 (0.872 to 1.002)
CD64 on CD14+ CD16+ monocyte	11	MR Egger	0.879	0.972 (0.678 to 1.393)
	11	Weighted median	0.097	0.827 (0.661 to 1.035)
	11	Inverse variance weighted	**0.015**	0.822 (0.702 to 0.963)
	11	Simple mode	0.144	0.757 (0.536 to 1.068)
	11	Weighted mode	0.203	0.793 (0.568 to 1.107)
CD80 on monocyte	20	MR Egger	0.205	0.928 (0.831 to 1.037)
	20	Weighted median	0.204	0.939 (0.852 to 1.035)
	20	Inverse variance weighted	**0.029**	0.922 (0.857 to 0.991)
	20	Simple mode	0.485	0.953 (0.835 to 1.088)
	20	Weighted mode	0.407	0.953 (0.853 to 1.065)
FSC−A on CD14+ monocyte	23	MR Egger	0.185	0.937 (0.854 to 1.028)
	23	Weighted median	0.084	0.912 (0.822 to 1.012)
	23	Inverse variance weighted	**0.021**	0.925 (0.865 to 0.988)
	23	Simple mode	0.345	0.928 (0.798 to 1.080)
	23	Weighted mode	0.081	0.922 (0.846 to 1.006)
HVEM on CD45RA− CD4+	18	MR Egger	0.154	0.919 (0.823 to 1.027)
	18	Weighted median	0.424	0.962 (0.875 to 1.058)
	18	Inverse variance weighted	**0.009**	0.924 (0.871 to 0.981)
	18	Simple mode	0.703	0.968 (0.823 to 1.139)
	18	Weighted mode	0.562	0.970 (0.876 to 1.073)
IgD− CD38− %B cell	11	MR Egger	0.742	1.044 (0.812 to 1.343)
	11	Weighted median	0.204	1.125 (0.938 to 1.350)
	11	Inverse variance weighted	**0.045**	1.156 (1.003 to 1.331)
	11	Simple mode	0.385	1.137 (0.862 to 1.500)
	11	Weighted mode	0.413	1.093 (0.891 to 1.341)
Plasmacytoid DC %DC	24	MR Egger	0.375	0.952 (0.855 to 1.060)
	24	Weighted median	0.219	0.943 (0.858 to 1.036)
	24	Inverse variance weighted	**0.042**	0.929 (0.865 to 0.997)
	24	Simple mode	0.304	0.915 (0.775 to 1.080)
	24	Weighted mode	0.259	0.949 (0.887 to 1.037)
SSC−A on CD14+ monocyte	21	MR Egger	0.705	1.025 (0.904 to 1.162)
	21	Weighted median	0.066	1.105 (0.993 to 1.230)
	21	Inverse variance weighted	**0.015**	1.101 (1.019 to 1.189)
	21	Simple mode	0.148	1.180 (0.951 to 1.463)
	21	Weighted mode	0.075	1.120 (0.995 to 1.259)
SSC−A on monocyte	21	MR Egger	0.090	1.106 (0.990 to 1.235)
	21	Weighted median	0.074	1.062 (0.992 to 1.179)
	21	Inverse variance weighted	**0.009**	1.099 (1.021 to 1.160)
	21	Simple mode	0.188	1.099 (0.960 to 1.257)
	21	Weighted mode	0.058	1.092 (1.002 to 1.189)
T/B	26	MR Egger	0.137	0.897 (0.782 to 1.030)
	26	Weighted median	0.253	0.934 (0.832 to 1.050)
	26	Inverse variance weighted	**0.027**	0.918 (0.852 to 0.990)
	26	Simple mode	0.746	0.968 (0.796 to 1.177)
	26	Weighted mode	0.489	0.948 (0.817 to 1.100)
TD CD4+ %CD4+	20	MR Egger	0.060	0.790 (0.628 to 0.994)
	20	Weighted median	0.293	0.919 (0.785 to 1.076)
	20	Inverse variance weighted	**0.037**	0.888 (0.794 to 0.993)
	20	Simple mode	0.454	0.909 (0.712 to 1.161)
	20	Weighted mode	0.199	0.876 (0.722 to 1.065)

FIGURE 6
Forest plot for MR analysis with rectal cancer as the outcome.

monocyte" (IVW p=0.0154; OR=0.822, 95%CI[0.702 ~ 0.963]), "CD25 on activated Treg" (IVW p=0.005; OR=0.845, 95%CI [0.752 ~ 0.951]), and "TD CD4+ %CD4+" (IVW p=0.037; OR=0.888, 95%ci[0.794 ~ 0.993]). The heterogeneity of these three factors was evaluated by IVW test, with corresponding Q *p* values of 0.491, 0.544, and 0.301, and by Egger test, with Q *p* values of 0.492, 0.511, and 0.320 respectively (Supplementary Figure 6A). On the other hand, the top three immune traits with the highest ORs were "CD4+ %leukocyte" (IVW p=0.049; OR=1.160, 95%CI [1.001 ~ 1.345]), "IgD- CD38- %B cell" (IVW p=0.045; OR=1.156, 95%CI[1.003 ~ 1.331]), and "SSC-A on CD14+ monocyte" (IVW p=0.015; OR=1.101, 95%ci[1.019 ~ 1.189]). The heterogeneity of these identified risk factors was also evaluated by IVW test, with corresponding Q *p* values of 0.749, 0.394, and 0.632, and MR Egger test, with values of 0.747, 0.386, and 0.701 (Supplementary Figure 6A). Furthermore, Supplementary Figure 6B displays Egger intercepts, indicating the absence of significant pleiotropy, while leave-one-out analysis suggests the results are not influenced by the inclusion of any single SNP (Supplementary Figure 6C).

3.6 Exploring immune traits causally related to gastrointestinal tract cancers of different sites

In this study, we intersected immune traits causally related to gastrointestinal tract cancers of different sites with those previously identified (Figure 7). While no immune traits were found to be causally related to the occurrence of all five types of tumors, this study has identified seven immune traits as causally related to the occurrence of two or more types of tumors. Specifically, "CCR2 on CD14- CD16+ monocyte" was found to have a causal relationship with both stomach cancer and rectal cancer. "CD45 on CD4+" was identified to be causally related to both stomach cancer and colon cancer. Moreover, "CD28 on CD39+ activated Treg" was causally related to stomach cancer and esophageal cancer, while "CD19 on IgD+ CD38- naive" was found to be causally related to colon cancer and cancer of the small intestine. The study also revealed that "CD25hi CD45RA+ CD4 not Treg AC" was causally related to rectal cancer and colon cancer, and "CD27 on unsw mem" to rectal cancer and cancer of the small intestine. It is noteworthy that CD19 on IgD+ CD38- was found to be causally related to esophageal cancer, colon cancer, and cancer of the small intestine. We validated our results using the BioBank Japan (BBJ) database (https://biobankjp.org/en/index.html). Since data for esophageal cancer, gastric cancer, and colon cancer are only available in the BBJ database, we verified "CD45 on CD4+" and "CD28 on CD39+ activated Treg" only. Detailed MR analysis results can be found in Supplementary Table 4. The validation results from the BBJ database are consistent with our research findings.

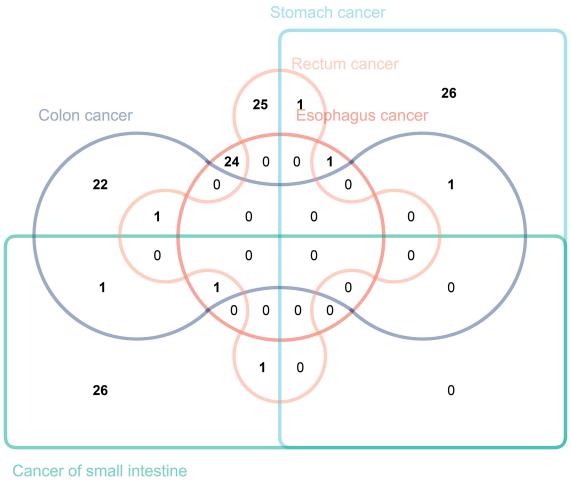

FIGURE 7
The Venn diagram illustrating the number of immune traits causally associated with various gastrointestinal tract tumors.

4 Discussion

In our study, we conducted a comprehensive analysis of 731 distinct immune traits to identify and screen for immune traits causally associated with different gastrointestinal tract cancers. From this analysis, we identified seven distinct immune traits that were causally linked to various cancers. This research not only strengthens the existing body of knowledge regarding the essential role of immune cells in the development and progression of cancers, but also provides fundamental insights and a new perspective on the prevention and treatment of tumors, and the development of novel anti-cancer therapies.

It is noteworthy that nearly all MR analysis methodologies have suggested a protective role of plasmacytoid dendritic cells (pDCs) against esophageal cancer. Previous studies have demonstrated that pDCs represent a subtype of dendritic cells that can generate copious amounts of type I interferon (IFN-I/α) (30). Under normal conditions, TLR-activated pDCs produce potent IFN-α, thereby promoting both innate and adaptive immune responses. However, within the context of cancer, the activation response of pDCs to TLR7/9 is impaired, resulting in decreased or absent production of IFN-α, which in turn, leads to the establishment of an immunosuppressive tumor microenvironment (31). Beyond their production of IFN-α, pDCs also function as antigen-presenting cells (APCs), regulating immune responses to various antigens (32). While clinical trial outcomes of DC-based vaccines have proved disappointing, recent research has underscored the pivotal role of DC-mediated cross-priming in eliciting anti-tumor CD8 T cell immunity and modulating the anti-tumor effects of immunotherapies. Consequently, these emerging findings advocate for further advancement and refinement of DC-based vaccines, positioning them as standalone immunotherapies or in combination with other immunotherapies (33). Given pDCs' critical role in modulating both innate and adaptive components of the immune system, they are poised to play a central role in cancer immunology.

Moreover, within the small intestine, four of five MR-based analytical methods indicate a significant increase in cancer incidence risk associated with CD14+CD16− monocytes. CD14+ CD16- monocytes, classified as classical monocytes due to their

high CD14 expression and lack of CD16 expression, have been shown in previous studies to possess the capacity to secrete elevated levels of cytokines, including IL-6, CCL2, and G-CSF (34, 35). Among these cytokines, IL-6 is a major cytokine present in the tumor microenvironment and is overexpressed in almost all types of tumors. IL-6 promotes cancer progression by regulating tumor markers and multiple signaling pathways, including apoptosis, survival, proliferation, angiogenesis, invasion, and metastasis, as well as metabolism (36, 37). CCL2 is able to promote cancer cell growth and proliferation through various mechanisms. By interacting with CCR2, CCL2 facilitates cancer cell migration and recruits immunosuppressive cells to the tumor microenvironment, thereby promoting cancer development (38). Numerous preclinical investigations have elucidated the tumor-promoting impact of granulocyte colony-stimulating factor (G-CSF), predominantly orchestrated by neutrophils and MDSCs, the primary subset expressing G-CSF receptors. In the presence of tumor-derived or exogenous G-CSF, these myeloid cell populations typically demonstrate a T-cell suppressive phenotype (39). Consequently, the high levels of cytokines secreted by CD14+ CD16- monocytes partly explain the tumor risks associated with these cells.

The MR analysis in this study suggests that CD4+ T cells serve as a protective factor against rectum cancer. Previous investigation have revealed that CD4+ T cells not only express key molecules associated with cytolysis (such as Granzymes [GZM] and Perforin [PRF1]) but also possess direct cytotoxicity, forming the basis for their protective immunity, including in cancer (40). CD4+ T cells can engage tumor cells through various mechanisms, either by directly eliminating tumor cells via cytolysis or indirectly by modulating the tumor microenvironment (41). Additionally, in secondary lymphoid organs, CD4+ T cells amplify the intensity and quality of B cell and Cytotoxic T lymphocytes (CTLs) responses. Antigen-specific interaction with CD4+ T cells enables dendritic cells (DCs) to optimize antigen presentation and deliver specific cytokine and co-stimulatory signals to CD8+ T cells, facilitating their clonal expansion and differentiation into effector or memory T cells (40, 42). CD4+ T cells assist in initiating the gene expression program of CD8+ T cells, which enhances CTL function through various molecular mechanisms, enabling them to overcome obstacles commonly encountered in anticancer immunity (43).

CD19, a CD molecule expressed by B cells, is utilized within this signature to evaluate the level of IgD+ CD38- B cells based on fluorescence intensities in "CD19 on IgD+ CD38-" signature. As a subtype of Naive B cells, IgD+ CD38- B cells are suggested, based on MR analysis, to have a causal relationship with three types of gastrointestinal tract cancers (44). Naive B cells, referring to immature B lymphocytes that have yet to experience antigenic stimulation, are included within this B cell subset (45). These cells typically reside within lymphoid tissues, the spleen, and bone marrow, with a relatively short lifespan but the potential to react to a broad spectrum of antigens. Upon encountering specific antigens within lymphoid tissues during an infection, they receive assistance from T cells for differentiation and antibody production to combat the invading pathogen (46). Therefore, Naive B cells represent a highly significant group of immune cells that form the foundation of immune defense enabling the body to fend off diverse infections and pathogens. The precise mechanisms underlying the role of Naive B cells in the development of gastrointestinal tumors remain incompletely explained. However, this study has partially illuminated their crucial role in tumor occurrence, through the application of MR analysis.

In recent years, there has been a surge of interest in exploring the development of anti-cancer drugs targeting immune cells. Research has demonstrated that immune infiltration within the tumor microenvironment plays a critical role in the development and progression of cancer, ultimately affecting clinical outcomes in cancer patients (47). Several immunotherapies, including adoptive cell transfer (ACT) and immune checkpoint inhibitors (ICIs), have achieved persistent clinical responses, yet their efficacy varies and only a subset of cancer patients benefits from them (48–51). Therefore, a comprehensive analysis of the immune cells infiltrating the tumor will help elucidate the mechanisms underlying tumor immune evasion, ultimately providing opportunities for the development of novel therapeutic strategies (51–53). This study utilized MR analysis to screen and identify immune cells causally linked to gastrointestinal tract cancers, therefore providing novel potential therapeutic targets for immunotherapy and informing the development of targeted prevention and treatment strategies.

Our study has some limitations that should be taken into careful consideration. Firstly, despite conducting multiple sensitivity analyses, it was challenging to fully assess the extent of multiple horizontal pleiotropy. Additionally, due to the lack of access to more detailed clinical information for all individuals included in the analysis, we were unable to perform further stratified analyses on the study population. Furthermore, since our MR analysis was based on publicly available databases of European ancestry, the generalizability of our findings to other populations needs to be treated with caution. Then, in order to comprehensively describe, identify, and screen immune traits causally linked to gastrointestinal tract cancers, we used relatively lenient thresholds to assess our findings, which may increase the risk of false positives. Finally, our MR analysis results did not identify immune traits causally linked to the onset of gastrointestinal tumors across all sites, which may indirectly suggest substantial heterogeneity among gastrointestinal tumors at different locations and considerable divergence in immune factors associated with their onset. Nevertheless, our study comprehensively evaluated the causal relationships between various immune traits and the onset of gastrointestinal tumors at different sites, providing valuable resources and insights for further exploration of future immunotherapeutic strategies.

5 Conclusions

In conclusion, our comprehensive MR analysis has furnished substantiation for the existence of causal links between diverse immune traits and gastrointestinal tract cancers. This revelation not only expands the horizons for investigators delving into the intricate biological underpinnings of gastrointestinal tract cancers but also plays a pivotal role in advancing our understanding of strategies for prevention and management in this context.

Data availability statement

The original contributions presented in the study are included in the article/Supplementary Material. Further inquiries can be directed to the corresponding authors.

Ethics statement

The availability of large-scale genomic data from publicly accessible databases, such as the FinnGen and GWAS Catalog, has facilitated the use of such data in genetic epidemiology research. As the data used in our study were obtained from these publicly accessible databases and do not contain any identifiable information, it was deemed unnecessary for approval from a medical ethics committee board. Our study adhered to all relevant laws and regulations regarding the use of human genetic data, and we aim to promote open access of genetic data to facilitate scientific discoveries in the field of genetics.

Author contributions

Y-XW: Conceptualization, Data curation, Formal analysis, Funding acquisition, Writing – original draft. C-PZ: Investigation, Methodology, Project administration, Resources, Writing – review & editing. D-TW: Software, Supervision, Validation, Visualization, Writing – review & editing. JM: Conceptualization, Investigation, Software, Writing – review & editing. X-HS: Data curation, Methodology, Supervision, Writing – review & editing. YW: Formal analysis, Project administration, Validation, Writing – original draft. Y-MZ: Funding acquisition, Resources, Visualization, Writing – review & editing.

Funding

The author(s) declare that no financial support was received for the research, authorship, and/or publication of this article.

Conflict of interest

The authors declare that the research was conducted in the absence of any commercial or financial relationships that could be construed as a potential conflict of interest.

Publisher's note

Supplementary material

The Supplementary Material for this article can be found online at: https://www.frontiersin.org/articles/10.3389/fimmu.2024.1343512/full#supplementary-material

SUPPLEMENTARY FIGURE 1
The immune traits with *p*-values less than 0.05 obtained by the IVW method in esophageal cancer **(A)**, gastric cancer **(B)**, small intestine cancer **(C)**, colon cancer **(D)**, and rectal cancer **(E)**.

SUPPLEMENTARY FIGURE 2
The funnel plot **(A)**, scatter plot **(B)**, and leave-one-out sensitivity analysis for three immune traits with the maximum and minimum ORs associated with esophagus cancer.

SUPPLEMENTARY FIGURE 3
The funnel plot **(A)**, scatter plot **(B)**, and leave-one-out sensitivity analysis for three immune traits with the maximum and minimum ORs associated with stomach cancer.

SUPPLEMENTARY FIGURE 4
The funnel plot **(A)**, scatter plot **(B)**, and leave-one-out sensitivity analysis for three immune traits with the maximum and minimum ORs associated with cancer of small intestine.

SUPPLEMENTARY FIGURE 5
The funnel plot **(A)**, scatter plot **(B)**, and leave-one-out sensitivity analysis for three immune traits with the maximum and minimum ORs associated with colon cancer.

SUPPLEMENTARY FIGURE 6
The funnel plot **(A)**, scatter plot **(B)**, and leave-one-out sensitivity analysis for three immune traits with the maximum and minimum ORs associated with rectal cancer.

SUPPLEMENTARY TABLE 1
The information of 731 immunophenotypes in the GWAS Catalog.

SUPPLEMENTARY TABLE 2
The number of patients, and the URL for downloading the data for each type of gastrointestinal tract cancer.

SUPPLEMENTARY TABLE 3
The IVs associated with different immune traits.

SUPPLEMENTARY TABLE 4
The validation results from the BBJ database.

References

1. Ben-Aharon I, van Laarhoven H, Fontana E, Obermannova R, Nilsson M, Lordick F. Early-onset cancer in the gastrointestinal tract is on the rise-evidence and implications. *Cancer Discov.* (2023) 13:538–51. doi: 10.1158/2159-8290.CD-22-1038

2. Mantese G. Gastrointestinal stromal tumor: epidemiology, diagnosis, and treatment. *Curr Opin Gastroenterol.* (2019) 35:555–9. doi: 10.1097/MOG.0000000000000584

3. Poorolajal J, Moradi L, Mohammadi Y, Cheraghi Z, Gohari-Ensaf F. Risk factors for stomach cancer: a systematic review and meta-analysis. *Epidemiol Health*. (2020) 42:e2020004. doi: 10.4178/epih.e2020004

4. Miao L, Qi J, Zhao Q, Wu QN, Wei DL, Wei XL, et al. Targeting the STING pathway in tumor-associated macrophages regulates innate immune sensing of gastric cancer cells. *Theranostics*. (2020) 10(2):498–515. doi: 10.7150/thno.37745

5. Hoft SG, Pherson MD, DiPaolo RJ. Discovering immune-mediated mechanisms of gastric carcinogenesis through single-cell RNA sequencing. *Front Immunol*. (2022) 13:902017. doi: 10.3389/fimmu.2022.902017

6. Ruan H, Leibowitz BJ, Zhang L, Yu J. Immunogenic cell death in colon cancer prevention and therapy. *Mol Carcinog*. (2020) 59:783–93. doi: 10.1002/mc.23183

7. Shin JH, Jeong J, Maher SE, Lee HW, Lim J, Bothwell A. Colon cancer cells acquire immune regulatory molecules from tumor-infiltrating lymphocytes by trogocytosis. *Proc Natl Acad Sci USA*. (2021) 118:e2110241118. doi: 10.1073/pnas.2110241118

8. Zheng Y, Chen Z, Han Y, Han L, Zou X, Zhou B, et al. Immune suppressive landscape in the human esophageal squamous cell carcinoma microenvironment. *Nat Commun*. (2020) 11(1):6268. doi: 10.1038/s41467-020-20019-0

9. Lou Q, Liu R, Yang X, Li W, Huang L, Wei L, et al. miR-448 targets IDO1 and regulates CD8+ T cell response in human colon cancer. *J Immunother Cancer*. (2019) 7 (1):210. doi: 10.1186/s40425-019-0691-0

10. Kitagawa Y, Akiyoshi T, Yamamoto N, Mukai T, Hiyoshi Y, Yamaguchi T, et al. Tumor-infiltrating PD-1+ Immune cell density is associated with response to neoadjuvant chemoradiotherapy in rectal cancer. *Clin Colorectal Cancer*. (2022) 21 (1):e1–e11. doi: 10.1016/j.clcc.2022.01.004

11. Derynck R, Turley SJ, Akhurst RJ. TGFβ biology in cancer progression and immunotherapy. *Nat Rev Clin Oncol*. (2021) 18:9–34. doi: 10.1038/s41571-020-0403-1

12. Li K, Zhang A, Li X, Zhang H, Zhao L. Advances in clinical immunotherapy for gastric cancer. *Biochim Biophys Acta Rev Cancer*. (2021) 1876:188615. doi: 10.1016/j.bbcan.2021.188615

13. Sekula P, Del Greco MF, Pattaro C, Köttgen A. Mendelian randomization as an approach to assess causality using observational data. *J Am Soc Nephrol*. (2016) 27:3253–65. doi: 10.1681/ASN.2016010098

14. Birney E. Mendelian randomization. *Cold Spring Harb Perspect Med*. (2022) 12: a041302. doi: 10.1101/cshperspect.a041302

15. Wang C, Zhu D, Zhang D, Zuo X, Yao L, Liu T, et al. Causal role of immune cells in schizophrenia: Mendelian randomization (MR) study. *BMC Psychiatry*. (2023) 23 (1):590. doi: 10.1186/s12888-023-05081-4

16. Yin KJ, Huang JX, Wang P, Yang XK, Tao SS, Li HM, et al. No genetic causal association between periodontitis and arthritis: A bidirectional two-sample mendelian randomization analysis. *Front Immunol*. (2022) 13:808832. doi: 10.3389/fimmu.2022.808832

17. Gao N, Kong M, Li X, Wei D, Zhu X, Hong Z, et al. Systemic lupus erythematosus and cardiovascular disease: A mendelian randomization study. *Front Immunol*. (2022) 13:908831. doi: 10.3389/fimmu.2022.908831

18. Xiang M, Wang Y, Gao Z, Wang J, Chen Q, Sun Z, et al. Exploring causal correlations between inflammatory cytokines and systemic lupus erythematosus: A Mendelian randomization. *Front Immunol*. (2023) 13:985729. doi: 10.3389/fimmu.2022.985729

19. Kurki MI, Karjalainen J, Palta P, Sipil TP, Kristiansson K, Donner KM, et al. FinnGen provides genetic insights from a well-phenotyped isolated population. *Nature*. (2023) 613(7944):508–18. doi: 10.1038/s41586-022-05473-8

20. Guo YG, Zhang Y, Liu WL. The causal relationship between allergic diseases and heart failure: Evidence from Mendelian randomization study. *PloS One*. (2022) 17: e0271985. doi: 10.1371/journal.pone.0271985

21. Burgess S, Butterworth A, Thompson SG. Mendelian randomization analysis with multiple genetic variants using summarized data. *Genet Epidemiol*. (2013) 37:658–65. doi: 10.1002/gepi.21758

22. Li P, Wang H, Guo L, Gou X, Chen G, Lin D, et al. Association between gut microbiota and preeclampsia-eclampsia: a two-sample Mendelian randomization study. *BMC Med*. (2022) 20(1):443. doi: 10.1186/s12916-022-02657-x

23. Ni JJ, Xu Q, Yan SS, Han BX, Zhang H, Wei XT, et al. Gut microbiota and psychiatric disorders: A two-sample mendelian randomization study. *Front Microbiol*. (2022) 12:737197. doi: 10.3389/fmicb.2021.737197

24. Chen X, Tang H, Lin J, Zeng R. Causal relationships of obesity on musculoskeletal chronic pain: A two-sample Mendelian randomization study. *Front Endocrinol (Lausanne)*. (2022) 13:971997. doi: 10.3389/fendo.2022.971997

25. Wang Q, Qi Y, Li Y, Yan Z, Wang X, Ma Q, et al. Psychiatric traits and intracerebral hemorrhage: A Mendelian randomization study. *Front Psychiatry*. (2023) 13:1049432. doi: 10.3389/fpsyt.2022.1049432

26. Yang M, Xu J, Zhang F, Luo P, Xu K, Feng R, et al. Large-scale genetic correlation analysis between spondyloarthritis and human blood metabolites. *J Clin Med*. (2023) 12 (3):1201. doi: 10.3390/jcm12031201

27. Yang M, Wan X, Zheng H, Xu K, Xie J, Yu H, et al. No evidence of a genetic causal relationship between ankylosing spondylitis and gut microbiota: A two-sample mendelian randomization study. *Nutrients*. (2023) 15(4):1057. doi: 10.3390/nu15041057

28. Zhou H, Zhang Y, Liu J, Yang Y, Fang W, Hong S, et al. Education and lung cancer: a Mendelian randomization study. *Int J Epidemiol*. (2019) 48(3):743–50. doi: 10.1093/ije/dyz121

29. Lu H, Wu PF, Zhang W, Liao X. Circulating interleukins and risk of multiple sclerosis: A mendelian randomization study. *Front Immunol*. (2021) 12:647588. doi: 10.3389/fimmu.2021.647588

30. Swiecki M, Colonna M. The multifaceted biology of plasmacytoid dendritic cells. *Nat Rev Immunol*. (2015) 15:471–85. doi: 10.1038/nri3865

31. Croft W, Evans R, Pearce H, Elshafie M, Griffiths EA, Moss P. The single cell transcriptional landscape of esophageal adenocarcinoma and its modulation by neoadjuvant chemotherapy. *Mol Cancer*. (2022) 21:200. doi: 10.1186/s12943-022-01666-x

32. Mitchell D, Chintala S, Dey M. Plasmacytoid dendritic cell in immunity and cancer. *J Neuroimmunol*. (2018) 322:63–73. doi: 10.1016/j.jneuroim.2018.06.012

33. Fu C, Zhou L, Mi QS, Jiang A. Plasmacytoid dendritic cells and cancer immunotherapy. *Cells*. (2022) 11:222. doi: 10.3390/cells11020222

34. Ożańska A, Szymczak D, Rybka J. Pattern of human monocyte subpopulations in health and disease. *Scand J Immunol*. (2020) 92:e12883. doi: 10.1111/sji.12883

35. Sampath P, Moideen K, Ranganathan UD, Bethunaickan R. Monocyte subsets: phenotypes and function in tuberculosis infection. *Front Immunol*. (2018) 9:1726. doi: 10.3389/fimmu.2018.01726

36. Kumari N, Dwarakanath BS, Das A, Bhatt AN. Role of interleukin-6 in cancer progression and therapeutic resistance. *Tumour Biol*. (2016) 37:11553–72. doi: 10.1007/s13277-016-5098-7

37. Naqash AR, McCallen JD, Mi E, Iivanainen S, Marie MA, Gramenitskaya D, et al. Increased interleukin-6/C-reactive protein levels are associated with the upregulation of the adenosine pathway and serve as potential markers of therapeutic resistance to immune checkpoint inhibitor-based therapies in non-small cell lung cancer. *J Immunother Cancer*. (2023) 11(10):e007310. doi: 10.1136/jitc-2023-007310

38. Xu M, Wang Y, Xia R, Wei Y, Wei X. Role of the CCL2-CCR2 signalling axis in cancer: Mechanisms and therapeutic targeting. *Cell Prolif*. (2021) 54:e13115. doi: 10.1111/cpr.13115

39. Mouchemore KA, Anderson RL. Immunomodulatory effects of G-CSF in cancer: Therapeutic implications. *Semin Immunol*. (2021) 54:101512. doi: 10.1016/j.smim.2021.101512

40. Oh DY, Fong L. Cytotoxic CD4(+) T cells in cancer: Expanding the immune effector toolbox. *Immunity*. (2021) 54:2701–11. doi: 10.1016/j.immuni.2021.11.015

41. Borst J, Ahrends T, Bąbała N, Melief C, Kastenmüller W. CD4(+) T cell help in cancer immunology and immunotherapy. *Nat Rev Immunol*. (2018) 18:635–47. doi: 10.1038/s41577-018-0044-0

42. Wang B, Hu S, Fu X, Li L. CD4(+) cytotoxic T lymphocytes in cancer immunity and immunotherapy. *Adv Biol (Weinh)*. (2023) 7:e2200169. doi: 10.1002/adbi.202200169

43. Zander R, Schauder D, Xin G, Nguyen C, Wu X, Zajac A, et al. CD4+ T cell help is required for the formation of a cytolytic CD8+ T cell subset that protects against chronic infection and cancer. *Immunity*. (2019) 51(6):1028–1042.e4. doi: 10.1016/j.immuni.2019.10.009

44. Liechti T, Günthard HF, Trkola A. OMIP-047: High-Dimensional phenotypic characterization of B cells. *Cytometry A*. (2018) 93:592–6. doi: 10.1002/cyto.a.23488

45. Su KY, Watanabe A, Yeh CH, Kelsoe G, Kuraoka M. Efficient culture of human naive and memory B cells for use as APCs. *J Immunol*. (2016) 197:4163–76. doi: 10.4049/jimmunol.1502193

46. Weisel NM, Joachim SM, Smita S, Callahan D, Elsner RA, Conter LJ, et al. Surface phenotypes of naive and memory B cells in mouse and human tissues. *Nat Immunol*. (2022) 23(1):135–45. doi: 10.1038/s41590-021-01078-x

47. Xiao Y, Yu D. Tumor microenvironment as a therapeutic target in cancer. *Pharmacol Ther*. (2021) 221:107753. doi: 10.1016/j.pharmthera.2020.107753

48. Miller JS, Soignier Y, Panoskaltsis-Mortari A, McNearney SA, Yun GH, Fautsch SK, et al. Successful adoptive transfer and *in vivo* expansion of human haploidentical NK cells in patients with cancer. *Blood*. (2005) 105(8):3051–7. doi: 10.1182/blood-2004-07-2974

49. Qi C, Gong J, Li J, Liu D, Qin Y, Ge S, et al. Claudin18.2-specific CAR T cells in gastrointestinal cancers: phase 1 trial interim results. *Nat Med*. (2022) 28(6):1189–98. doi: 10.1038/s41591-022-01800-8

50. Li S, Yu W, Xie F, Luo H, Liu Z, Lv W, et al. Neoadjuvant therapy with immune checkpoint blockade, antiangiogenesis, and chemotherapy for locally advanced gastric cancer. *Nat Commun*. (2023) 14(1):8. doi: 10.1038/s41467-022-35431-x

51. Peyraud F, Guégan JP, Bodet D, Nafia I, Fontan L, Auzanneau C, et al. Circulating L-arginine predicts the survival of cancer patients treated with immune checkpoint inhibitors. *Ann Oncol*. (2022) 33(10):1041–51. doi: 10.1016/j.annonc.2022.07.001

52. Lee HW, Chung W, Lee HO, Jeong DE, Jo A, Lim JE, et al. Single-cell RNA sequencing reveals the tumor microenvironment and facilitates strategic choices to circumvent treatment failure in a chemorefractory bladder cancer patient. *Genome Med*. (2020) 12(1):47. doi: 10.1186/s13073-020-00741-6

53. Zeng D, Wu J, Luo H, Li Y, Xiao J, Peng J, et al. Tumor microenvironment evaluation promotes precise checkpoint immunotherapy of advanced gastric cancer. *J Immunother Cancer*. (2021) 9(8):e002467. doi: 10.1136/jitc-2021-002467